

FULL PAPER

Novel conjugated nanoporous alkynyl metalloporphyrin framework as effective catalyst for oxidation of toluene with molecular oxygen

Yongjin Li | Baoshuai Sun | Yuanrong Zhou | Weijun Yang*

Department of Chemistry and Chemical Engineering, Hunan University, Changsha 410082, Hunan, China

Correspondence

Weijun Yang, Department of Chemistry and Chemical Engineering, Hunan University, Changsha, 410082, Hunan, China.
Email: wjyang@hnu.edu.cn

A porous alkynylporphyrin conjugated organic polymer (MnE-TPP) was synthesized by Sonogashira coupling reaction with Mn(II) 5,10,15,20-tetrakis(4'-ethynylphenyl)porphyrin and Mn(II) 5,10,15,20-tetrakis(4'-bromophenyl)porphyrin as building blocks. The polymer was characterized using nitrogen adsorption-desorption isotherms, field-emission scanning electron microscopy, high-resolution transmission electron microscopy, Fourier transform infrared and UV-visible spectroscopies, X-ray diffraction, thermogravimetry and inductively coupled plasma atomic emission spectrometry. The electrochemical behaviors of MnE-TPP were investigated by cyclic voltammetry. MnE-TPP was developed as a heterogeneous catalyst for the activation of molecular oxygen to oxidize toluene under mild conditions. The selectivity of total benzaldehyde and benzyl alcohol remained above 70.0% with a conversion of toluene up to 10.2%. The turnover number was as high as 13 653. Also, MnE-TPP remained structurally stable and the toluene conversion rate hardly decreased after 5 h of reaction and five cycles of reuse.

KEYWORDS

alkynylporphyrin polymer, benzaldehyde, catalysis, oxidation, toluene

1 | INTRODUCTION

Benzaldehyde and benzyl alcohol are versatile intermediates in the chemical industry, and the selective oxidation of toluene with air is the most important way to synthesize them industrially.^[1,2] However, using this method it is easy to generate benzoic acid because of over-oxidation of benzaldehyde.^[3] Therefore, it is of great significance to develop highly selective catalysts for the oxidation of toluene into benzaldehyde and benzyl alcohol.

By activating oxygen molecules under mild conditions, cytochrome P450 enzyme functions as a highly active catalyst for oxidation reactions. Metalloporphyrin, which has a similar structure to the active center of cytochrome P450 enzyme, has been employed as a biomimetic catalyst for a variety of oxidation reactions.^[4–8] The aerobic oxidation of toluene has been catalyzed by metalloporphyrin to prepare benzaldehyde and benzyl alcohol.^[9–12] Although metalloporphyrin increases the conversion rate of toluene as

well as the selectivity of benzaldehyde and benzyl alcohol, many problems are still unsolved. For example, monomer metalloporphyrins can be separated with difficulty from solvents at the end of reaction, and they are prone to oxidative damage during the catalysis process and thus cannot be recycled, which limits their application in practical production. As a result, monomer metalloporphyrins have been immobilized on solid supports to improve stability, but the bond between porphyrin and solid support surface is not stable. In addition, the activity of supported metalloporphyrin declines soon with reuse.^[13]

Metalloporphyrin polymerization is another way to improve the stability of metalloporphyrins,^[14–16] such as in metalloporphyrin-based metal-organic frameworks (MOFs). In the structure of MOFs, metal ions at the *para*-position of the metalloporphyrin are bridge sites.^[17,18] High density of open metal sites within the highly ordered structure and confined nanospace make metalloporphyrin-based MOFs useful in the design of materials for gas storage, chemical

separations, light response, sensors and other applications.^[19–22] However, few catalytic metalloporphyrin-based MOFs have been reported, which suggests that this kind of polymerization with metallic ion bridges may weaken the catalytic activities of monomer metalloporphyrins.

Recently, monomeric iron porphyrin has been bridged by a conjugated phenyl group to form a new reusable conjugated porous porphyrin polymer catalyst.^[23,24] In the study reported here, on the basis of the geometric properties of porphyrin, Mn(II) 5,10,15,20-tetrakis(4'-ethynylphenyl)porphyrin ([p-ethynyl]₄PMn) and Mn(II) 5,10,15,20-tetrakis(4'-bromophenyl)porphyrin ([p-Br]₄PMn) were used as building blocks to synthesize a porous organic conjugated porphyrin polymer (MnE-TPP). Through the *para*-position coupling reaction, a super-conjugated metalloporphyrin polymer was synthesized with an alkynylphenyl conjugated bridge and a highly ordered, well-developed micro- and mesoporous structure. Unlike metalloporphyrins, homogeneous catalysts, MnE-TPP allowed heterogeneous catalysis and circumvented recycling issues in oxidation. The catalytic oxidation performance and recyclability of MnE-TPP were greatly improved. MnE-TPP in which porphyrin monomers are connected with stable covalent bonds was superior to supported porphyrin or porphyrin polymer with metal ion bridges. Hence, the polymer has the potential for reuse.

2 | EXPERIMENTAL

2.1 | Materials

The following chemicals were used: bromobenzaldehyde (99.77%, Aladdin Reagents (Shanghai) Co. Ltd), palladium

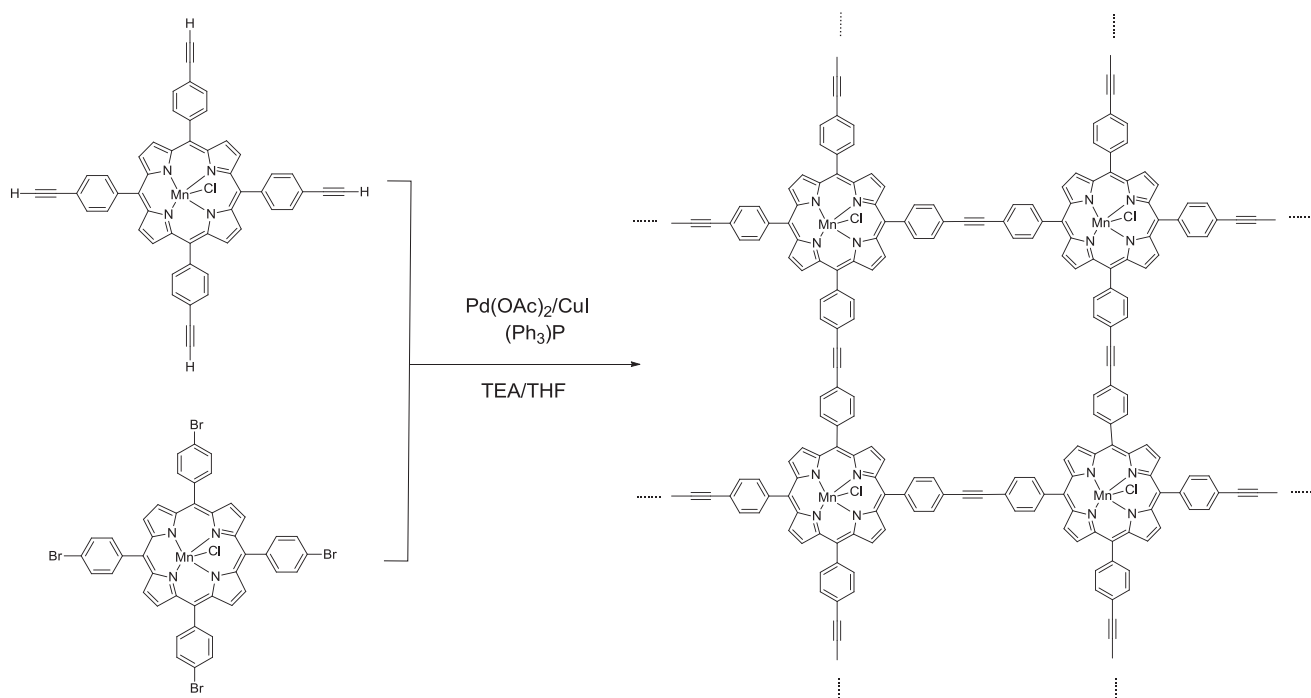
acetate (47.5% Pd, J&K Chemicals), trimethylsilylacetylene (98%, J&K Chemicals) and pyrrole (analytical grade, redistilled before use). Other organic reagents were of analytical grade and purchased from Aladdin Reagents (Shanghai) Co. Ltd without special treatment. [p-Br]₄PMn and [p-ethynyl]₄PMn were synthesized by our group according to documented procedures (supporting information).

2.2 | Synthesis of MnE-TPP

A mixture of [p-ethynyl]₄PMn (160 mg, 0.2 mmol), [p-Br]₄PMn (245 mg, 0.24 mmol), triphenylphosphine (105 mg, 0.4 mmol), palladium acetate (22.45 mg, 0.1 mmol) and copper iodide (38.09 mg, 0.2 mmol) was added into a 100 ml three-necked flask and air was removed by three cycles of argon gas pump-inflation. Air-removed tetrahydrofuran (THF; 9 ml) and triethylamine (TEA; 3 ml) were then injected into the three-necked flask under stirring and refluxed at 76°C for 3 h. Finally, the mixture was poured into plenty of deionized water after being cooled to room temperature. The solid crude product was then collected by filtration, and carefully washed in turn with water, THF, methanol and trichloromethane. It was also washed by Soxhlet extraction with water, THF, methanol and trichloromethane successively for 24 h, and then dried in vacuum, affording a dark green solid (MnE-TPP) with a yield of 90% (Scheme 1).

2.3 | Catalyst characterization

The specific surface area and pore size distribution were determined with a Beckman Coulter Inc. SA3100 accelerated surface and porosity analyzer with nitrogen as probing gas at 77 K. The specific surface areas were calculated using the



SCHEME 1 Synthesis of nanoporous polymer (MnE-TPP) with [p-ethynyl]₄PMn and [p-Br]₄PMn

Brunauer–Emmett–Teller (BET) method, and the NLDFT theory was utilized to estimate pore size, pore volume and pore distribution. Field-emission scanning electron microscopy (FE-SEM) images were recorded with a JEOL model JSM-5600Lv microscope. High-resolution transmission electron microscopy (HR-TEM) images were recorded with a JEOL model JEM-3010 microscope. Fourier transform infrared (FT-IR) spectra were obtained with a Shimadzu IR Prestige-21 spectrometer. UV–visible absorption spectra were obtained with an Agilent Cary 100 UV–visible spectrophotometer and diffuse reflectance spectra were obtained using the spectrophotometer equipped with integration sphere, and samples were diluted with BaSO₄. X-ray diffraction (XRD) examination was carried out using a Shimadzu 6100 instrument with Cu K α radiation operated at 40 kV and 30 mA.

2.4 | Cyclic voltammetry measurements of MnE-TPP

Electrochemical measurements of cyclic voltammetry were conducted using a CHI660B electrochemical workstation with a three-electrode cell system, in which a glassy carbon electrode, after loading the MnE-TPP, was used as the working electrode, a calomel electrode as the reference electrode and a Pt wire as the counter electrode. As to electrode preparation, the MnE-TPP sample was dispersed in 0.5 ml of solvent mixture containing 11 μ l of Nafion (5 wt%) and 0.49 ml of ethanol by sonication for more than 1 h to obtain a stable suspension. And then a 10 μ l portion of the sample solution was lightly dropped on the surface of the pre-polished glassy carbon electrode. The electrodes were dried overnight at room temperature for measurement. The electrochemical experiments were conducted in 0.1 mol l⁻¹ (CH₃CH₂)₄NBr CH₂Cl₂ solution. The experiments were cyclically scanned at a scan rate of 50 mV s⁻¹ at room temperature after purging with argon gas for 10 min.

2.5 | Catalytic oxidation of toluene

Toluene oxidation with air was catalyzed by MnE-TPP. Briefly, 200 ml of toluene and 10 mg of MnE-TPP were added into a 250 ml autoclave reactor, into which 0.6 MPa argon gas was injected before the toluene was heated to 160°C. After the reaction mixture was heated to 160°C along with stirring, air was injected at a speed of 1000 ml min⁻¹ while the pressure was kept at 0.6 MPa. The mixture was sampled every 30 min, and benzaldehyde and benzyl alcohol in the samples were analyzed by GC using chlorobenzene as internal standard. The contents of benzoic acid and ester were measured by chemical titration.^[25]

3 | RESULTS AND DISCUSSION

3.1 | MnE-TPP characterization

Nitrogen sorption isotherm measurements of MnE-TPP at 77 K display a typical type-III sorption isotherm curve along

with a strong adsorption at low pressure ($P/P_0 < 0.1$) (Figure 1(a)), suggesting coexistence of micropores and mesopores in the framework. The BET surface area is determined to be as high as 380 m² g⁻¹, and the main pore diameters are about 1.8 and 2.7 nm (Figure 1(b)). The contributions of 1.8 and 2.7 nm width pores to the pore volume are 38 and 62%, respectively, based on the cumulative pore volume profile. Therefore, MnE-TPP is an excellent microporous and mesoporous polymer.

As shown in Figure 2, the FT-IR spectrum of MnE-TPP is obviously different from that of [p-ethynyl]₄PMn. The characteristic peak of $\text{—C}\equiv\text{C—}$ at 2103 cm⁻¹ attenuates and even disappears because the structure of MnE-TPP is highly symmetric. The peak at 3292 cm⁻¹ in the spectrum of [p-ethynyl]₄PMn is assigned to C–H stretching, which disappears after formation of MnE-TPP due to the consumption of C–H. Meanwhile, an intense, broad peak at 3436 cm⁻¹, which typifies polyporphyrins, appears. On the other hand, the FT-IR spectrum of MnE-TPP exhibits a characteristic N–Mn vibration band at 1009 cm⁻¹, which is close to that

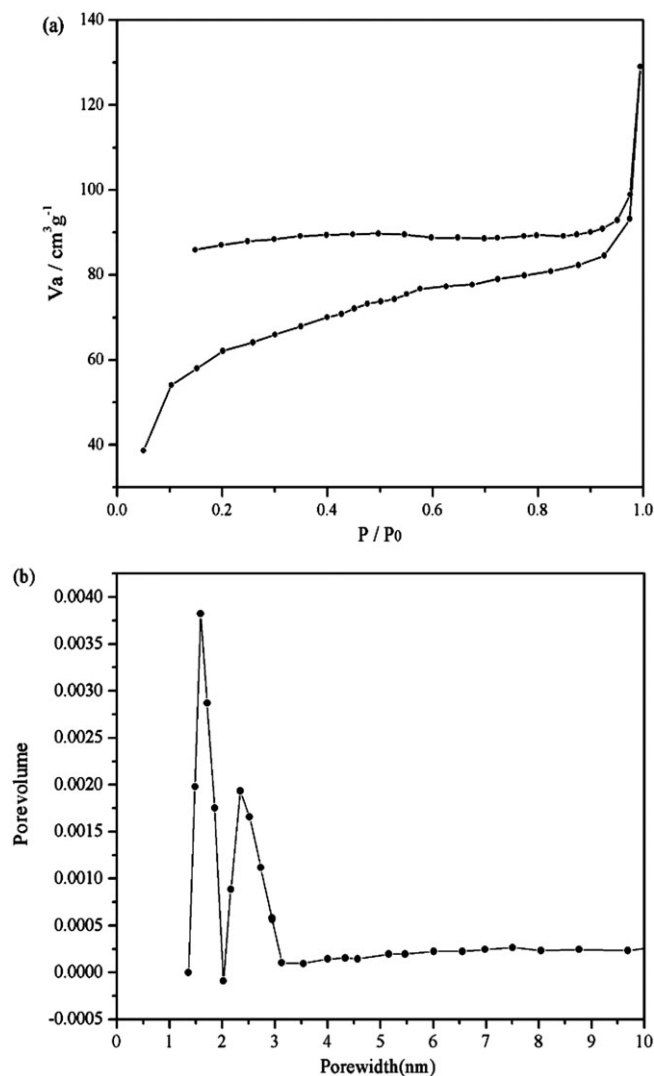


FIGURE 1 (a) Nitrogen adsorption and desorption isotherm profiles of MnE-TPP at 77 K. (b) Pore diameter examination of MnE-TPP

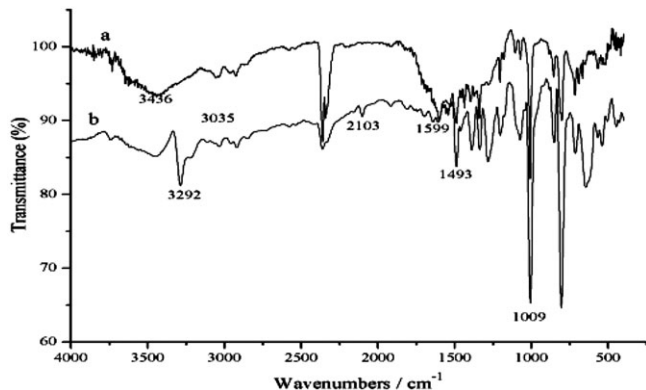


FIGURE 2 FT-IR spectra of (a) Mn-TPP and (b) [p-ethynyl]₄PMn

of [p-ethynyl]₄PMn (1001 cm⁻¹). The bands at 3035 and 1599 cm⁻¹ correspond to the C–H and C=C stretches in phenyls respectively, and that at 1493 cm⁻¹ represents the C=C stretch in porphyrin. Thus, [p-ethynyl]₄PMn had been introduced into the MnE-TPP porous structure in which manganese ion was still stably coordinated.

The morphology and crystallinity investigations of MnE-TPP were carried out using FE-SEM and HR-TEM. The FE-SEM images (Figures 3(a)–(c)) indicate that MnE-TPP comprises monoliths of about 1–2 μm originating from overlapping of circular flakes that are about 150–250 nm in diameter and 1–2 nm in thickness. Such a transition from a molecular-level framework to nanoscale layers and further to microscale monoliths resembles biological catalytic systems. The HR-TEM image (Figure 3(d)) shows that there are nanoholes on the surface of MnE-TPP.

The UV–visible spectra of MnE-TPP solid and of [p-ethynyl]₄PMn in CHCl₃ solution were also obtained (Figure 4). A strong absorption band at 480 nm is the Soret band of [p-ethynyl]₄PMn, and those at 580 and 620 nm are the Q-bands. MnE-TPP also shows the same typical UV–visible spectrum as that of [p-ethynyl]₄PMn, i.e. there are Soret bands at 462 and 496 nm and Q-bands at 582 and 622 nm. Compared with

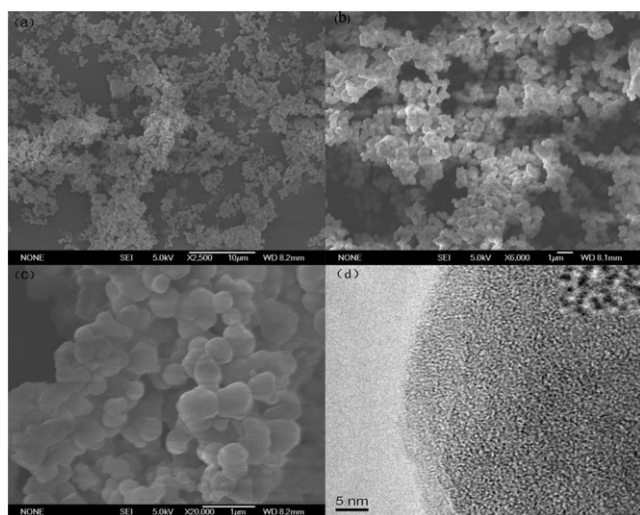


FIGURE 3 (a–c) FE-SEM images and (d) HR-TEM image of MnE-TPP

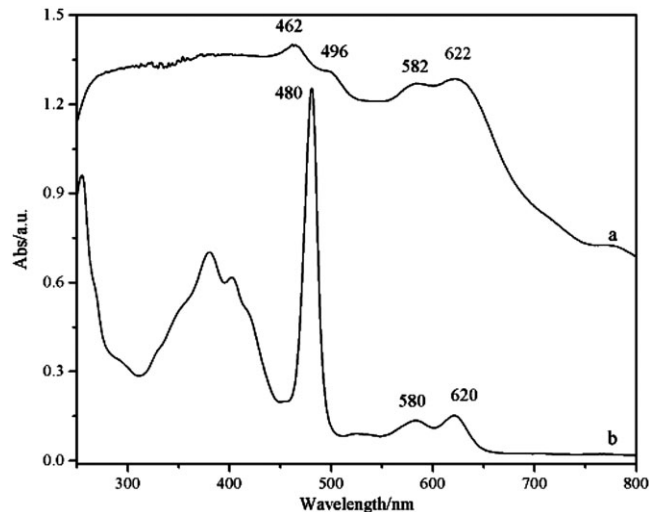


FIGURE 4 UV–visible spectra of (a) MnE-TPP (powder sample) and (b) [p-ethynyl]₄PMn (CHCl₃ solution)

[p-ethynyl]₄PMn monomer, the Soret band in MnE-TPP divides at 462 and 496 nm because of the electronic coupling effects of alkynyl between the porphyrin moieties in MnE-TPP.

Electrochemical measurements of cyclic voltammetry were also conducted. The first reduction potential of MnE-TPP is significantly right-shifted in comparison with the first reduction potential of [p-ethynyl]₄PMn (from –0.14 V to 0.04 V; Figure 5), which indicates that porphyrin monomers are bridged by the structure of –C≡C– in four directions of porphyrin rings.

The ethyne coupling units in MnE-TPP are hyperconjugated with porphyrin rings, thus allowing wide-

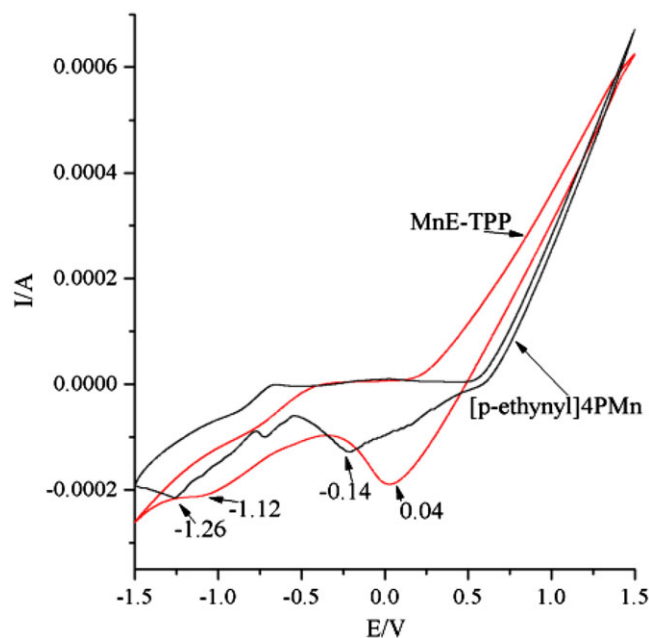


FIGURE 5 Cyclic voltammetry curves of MnE-TPP on glassy carbon electrodes in 0.1 mol l⁻¹ CH₂Cl₂ solution of (CH₃CH₂)₄NBr (red curve). Cyclic voltammetry curves of [p-ethynyl]₄PMn in mol l⁻¹ CH₂Cl₂ solution of (CH₃CH₂)₄NBr (black curve). Scan rate: 50 mV s⁻¹

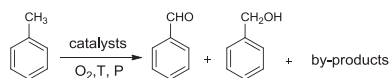
range flow of electrons and delocalization.^[26] The ethyne unit transfers electrons between the porphyrin units and thereby increases the energy-transfer rate in the macromolecule of MnE-TPP.^[27] As a result, Mn²⁺ ions in the center of porphyrin rings are further activated compared with those in the corresponding metalloporphyrin.

The bridge of alkynylphenyl in four directions of porphyrin rings allows MnE-TPP to be a highly ordered, highly developed microporous and mesoporous, and super-conjugated metalloporphyrin polymer. Hence, the catalytic oxidation activity of MnE-TPP towards C–H bond is significantly augmented. Furthermore, the XRD profile confirms the amorphous character of MnE-TPP (Figure S7). Owing to the covalent attachment and crosslinked structure, MnE-TPP is stable, and insoluble in water, dichloromethane, THF, acetone, methanol, dimethylsulfoxide and some other organic solvents. The thermal properties of MnE-TPP were characterized using thermogravimetric analysis (Figure S8). MnE-TPP is stable under 400°C and loses 72.4% of weight at 430°C, indicating that MnE-TPP is highly thermally stable. Accordingly, MnE-TPP should have excellent catalytic oxidation performance and favorable reusability.

3.2 | MnE-TPP as catalyst for toluene oxidation

MnE-TPP was then utilized as a new biomimetic catalyst for the oxidation of toluene in heterogeneous systems (Scheme 2). The catalytic oxidation results were compared with those for porphyrin monomers (Table 1).

Under MnE-TPP catalysis (Figure 6(a)), benzaldehyde, benzyl alcohol and benzoic acid continuously increase during 250 min of reaction, and the total yields of benzaldehyde and benzyl alcohol are higher than that of benzoic acid all the time. Starting from 210 min, increases of benzaldehyde yield slow down and the benzoic acid yield continues to grow. What is more, the yield of benzyl alcohol begins to decrease which means the deep oxidation of toluene, and the reaction is not conducive for producing benzaldehyde and benzyl



SCHEME 2 Oxidation of toluene catalyzed by MnE-TPP, [p-ethynyl]₄PMn and [p-Br]₄PMn catalysts

TABLE 1 Comparison of toluene oxidation catalyzed by various porphyrin catalysts^a

Catalyst	Selectivity (mol%)			Conversion (mol%)	Turnover (mol mol ⁻¹)
	Aldehyde	Alcohol	Acid		
MnE-TPP	42.2	27.8	16.7	10.2	13 653
[p-ethynyl] ₄ PMn	46.9	28.6	9.0	7.4	9 905
[p-Br] ₄ PMn	25.2	19.0	44.2	12.0	30 270

^aReaction conditions: toluene: 200 ml; catalyst: 10.0 mg; temperature: 160°C; pressure: 0.8 MPa; airflow: 1000 ml min⁻¹; time: 300 min.

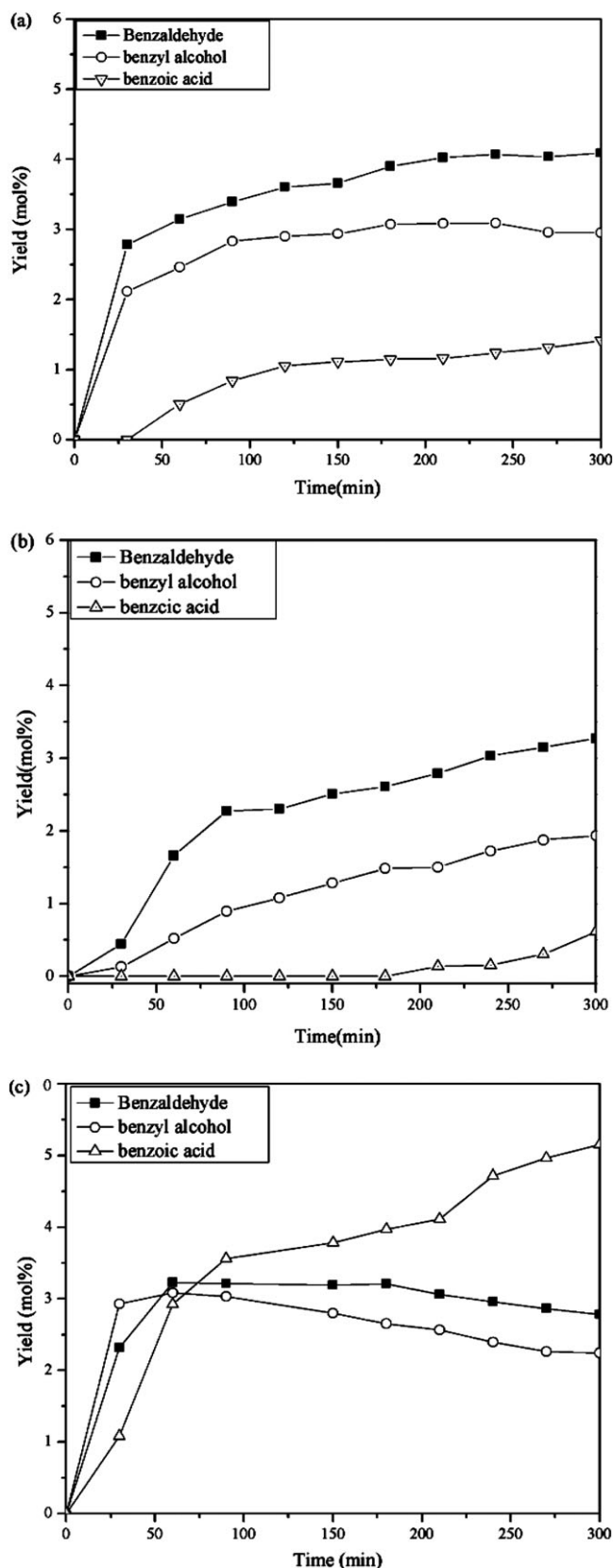


FIGURE 6 Distribution curves of reaction products in toluene oxidation catalyzed by (a) MnE-TPP, (b) [p-ethynyl]₄PMn and (c) [p-Br]₄PMn. Toluene: 200 ml; catalyst: 10.0 mg; temperature: 160°C; pressure: 0.8 MPa; airflow: 1000 ml min⁻¹; time: 300 min

alcohol. The total selectivity of benzaldehyde and benzyl alcohol is 73.5% and the conversion of toluene is 9.7% at 210 min.

When [p-ethynyl]₄PMn is employed as catalyst (Figure 6 (b)), no benzoic acid is generated within 180 min. Even at 300 min, benzoic acid only accounts for 9.0% of the products, and the total selectivity of benzaldehyde and benzyl alcohol is as high as 75.5%, but the conversion rate of toluene is just 7.4%. The reaction was so slow that there was little benzaldehyde and benzyl alcohol generated before 30 min. Although benzaldehyde increases rapidly and benzyl alcohol increases slowly at later time, the total yields of benzaldehyde and benzyl alcohol at 300 min (5.01%) are only similar to that of MnE-TPP as catalyst at 30 min (4.89%).

The total yields of benzaldehyde and benzyl alcohol, when toluene oxidation was catalyzed by [p-Br]₄PMn, increase rapidly to a plateau (5.24%) in about 30 min (Figure 6(c)). With increasing time to 90 min, the yield of benzoic acid exceeds those of benzaldehyde and benzyl alcohol and keeps rising significantly thereafter. Although the conversion rate of toluene is 12.0% at 300 min, the total selectivity of benzaldehyde and benzyl alcohol is, however, only 44.2%, which is much lower than that when MnE-TPP is used as catalyst (70%).

With MnE-TPP (Table 1) as catalyst, the total selectivity of benzaldehyde and benzyl alcohol is 70.0% at 10.2% conversion of toluene, with a turnover number of about 13 653 mol at 160°C, 0.6 MPa and 1000 ml min⁻¹ airflow rate. Under the same conditions, the selectivity of total benzaldehyde and benzyl alcohol is 75.5% when [p-ethynyl]₄PMn is used as the catalyst, but the conversion of toluene is only 7.4%. Although the conversion of toluene reaches 12.0% over [p-Br]₄PMn, the total selectivity of benzaldehyde and benzyl alcohol is only 44.2%. In comparison, Guo *et al.*^[9] reported that under catalysis of cobalt(II) tetraphenylporphyrin, the highest conversion rate of toluene was only 8.9%, and the maximum selectivity of total benzaldehyde and benzyl alcohol was just 60%. Hence, MnE-TPP, which was synthesized using [p-ethynyl]₄PMn and [p-Br]₄PMn, combines the advantages of the two during toluene catalytic oxidation, elevating the total selectivity of benzaldehyde and benzyl alcohol, also the conversion rate of toluene.

Moreover, as a porphyrin polymer with microporous conjugated structure, MnE-TPP is free from difficult recovery, high cost and oxidative damage during the heterogeneous catalytic oxidation of toluene. After the reaction, MnE-TPP can be directly recycled through centrifugation, filtration or some other simple methods. The reaction supernatant after the oxidation reaction was monitored using UV-visible spectrophotometry, which does not show the characteristic absorption bands of manganese porphyrin moiety or related decomposition products, which also indicates no degradation occurs in the oxidation reaction. After being recycled five times, the recovery of MnE-TPP reaches 90% and its BET surface area is 350 m² g⁻¹, being close to the initial value

(380 m² g⁻¹). In the meantime, the catalyst remains highly active under the optimized conditions. Particularly, the conversion rate of toluene exceeds 9.0%, and the total selectivity of benzaldehyde and benzyl alcohol remains basically unchanged. Since industrial costs can be reduced by continuing to increase the number of recycles, the catalyst is potentially applicable in industry.

4 | CONCLUSIONS

Single metal porphyrins are prone to loss of activity in homogeneous catalytic oxidation due to gradual oxidization and resulting in their single use. A metalloporphyrin conjugated polymer with [p-Br]₄PMn and [p-ethynyl]₄PMn as building blocks was synthesized in this work. With a porous structure and large BET surface area, MnE-TPP was highly catalytically active in toluene oxidation and could be reusable. Under MnE-TPP catalysis, the total selectivity of benzaldehyde and benzyl alcohol was 70.0% at 10.2% conversion of toluene, with a turnover numbers of about 13 653 mol at 160°C, 0.6 MPa and 1000 ml min⁻¹ airflow rate, combining the advantages of the two during catalytic toluene oxidation, elevating the conversion rate of toluene and the total selectivity of benzaldehyde and benzyl alcohol. In addition, the porphyrin polymer had a recovery rate of over 90%, thus meeting the requirements of modern green chemistry to replace porphyrins for catalytic oxidation of hydrocarbons, being potentially applicable to the industrial production of benzaldehyde and benzyl alcohol.

ACKNOWLEDGMENTS

The financial support of the National Natural Science Foundation of China (grant no. 21576074) is gratefully acknowledged. We are also grateful for the financial support of Hunan University.

REFERENCES

- [1] R. A. Sheldon, J. K. Kochi, *Metal-Catalyzed Oxidation of Organic Compounds*, Academic Press, New York **1981**.
- [2] F. M. Bautista, J. M. Campelo, D. Luna, J. Luque, J. M. Marin, *Appl. Catal. A* **2007**, 325, 336.
- [3] X. Q. Li, J. Xu, F. Wang, J. Gao, L. P. Zhou, G. Y. Yang, *Catal. Lett.* **2006**, 108, 137.
- [4] J. E. Falk, *Porphyrin and Metalloporphyrins*, ACT Press, Canberra **1953**.
- [5] F. Montanari, L. Casella, *Metalloporphyrin-Catalyzed Oxidation*, Academic Press, London **1994**.
- [6] C. C. Guo, G. Huang, X. B. Zhang, D. C. Guo, *Appl. Catal. A* **2003**, 247, 261.
- [7] P. E. Ellis, J. E. Lyons, *J. Chem. Soc., Chem. Commun.* **1989**, 1187.
- [8] W. J. Yang, B. J. Yin, C. C. Guo, Z. Tan, L. Zhang, *Chinese J. Catal.* **2010**, 31, 535.
- [9] C. C. Guo, Q. Liu, X. T. Wang, H. Y. Hu, *Appl. Catal. A* **2005**, 282, 55.
- [10] G. Huang, A. P. Wang, S. Y. Liu, Y. A. Guo, H. Zhou, S. K. Zhao, *Catal. Lett.* **2007**, 114, 174.
- [11] N. Taku, A. Noriko, K. Shiori, *Bull. Chem. Soc. Jpn.* **1996**, 69, 3513.
- [12] S. Evans, J. R. Lindsay Smith, *J. Chem. Soc. Perkin Trans. 2* **2000**, 1541.

- [13] G. Huang, J. Luo, C. C. Deng, Y. A. Guo, S. K. Zhao, H. Zhou, S. Wei, *Appl. Catal. A* **2008**, 338, 83.
- [14] A. Modak, J. Mondal, A. Bhaumik, *Appl. Catal. A* **2013**, 459, 41.
- [15] H. J. Mackintosh, P. M. Budd, N. B. Mckeown, *J. Mater. Chem.* **2008**, 18, 573.
- [16] N. B. McKeown, S. Hanif, K. Msayib, C. E. Tattershall, P. M. Budd, *Chem. Commun.* **2002**, 2782.
- [17] A. M. Shultz, O. K. Farha, J. T. Hupp, S. T. Nguyen, *J. Am. Chem. Soc.* **2009**, 131, 4204.
- [18] K. Suslick, P. Bhyrappa, J. H. Chou, M. E. Kosal, S. Nakagaki, D. W. Smithenry, S. R. Wilson, *Acc. Chem. Res.* **2005**, 38, 283.
- [19] X. S. Wang, L. Meng, Q. Cheng, C. Kim, L. Wojtas, M. Chrzanowski, Y. S. Chen, X. P. Zhang, S. Q. Ma, *J. Am. Chem. Soc.* **2011**, 133, 16322.
- [20] Z. J. Zhang, Y. G. Zhao, Q. H. Gong, Z. Li, J. Li, *Chem. Commun.* **2013**, 49, 653.
- [21] C. Y. Lee, O. K. Farha, B. J. Hong, A. A. Sarjeant, S. T. Nguyen, J. T. Hupp, *J. Am. Chem. Soc.* **2011**, 133, 15858.
- [22] O. K. Farha, A. M. Shultz, A. A. Sarjeant, S. T. Nguyen, J. T. Hupp, *J. Am. Chem. Soc.* **2011**, 133, 5652.
- [23] L. Chen, Y. Yang, D. L. Jiang, *J. Am. Chem. Soc.* **2010**, 132, 9138.
- [24] L. Chen, Y. Yang, Z. Q. Guo, D. L. Jiang, *Adv. Mater.* **2011**, 23, 3149.
- [25] W. W. Kaeding, R. O. Lindblom, R. G. Temple, H. I. Mahon, *Ind. Eng. Chem. Process Des. Dev.* **1965**, 4, 97.
- [26] H. L. Anderson, *Chem. Commun.* **1999**, 2323.
- [27] R. W. Wagner, T. E. Johnson, J. S. Lindsey, *J. Am. Chem. Soc.* **1996**, 118, 11166.

SUPPORTING INFORMATION

Additional supporting information can be found in the online version of this article at the publisher's website.

How to cite this article: Li, Y., Sun, B., Zhou, Y., and Yang, W. (2016), Novel conjugated nanoporous alkynyl metalloporphyrin framework as effective catalyst for oxidation of toluene with molecular oxygen, *Appl. Organometal. Chem.*, doi: 10.1002/aoc.3578